



University of Groningen

## First-order ferromagnetic transition in single-crystalline (Mn,Fe)(2)( P,Si)

Yibole, H.; Guillou, F.; Huang, Y. K.; Blake, G. R.; Lefering, A. J. E.; van Dijk, N. H.; Bruck, E.

*Published in:*  
Journal of Materials Research

*DOI:*  
[10.1063/1.4934500](https://doi.org/10.1063/1.4934500)

**IMPORTANT NOTE:** You are advised to consult the publisher's version (publisher's PDF) if you wish to cite from it. Please check the document version below.

*Document Version*  
Publisher's PDF, also known as Version of record

*Publication date:*  
2015

[Link to publication in University of Groningen/UMCG research database](#)

### *Citation for published version (APA):*

Yibole, H., Guillou, F., Huang, Y. K., Blake, G. R., Lefering, A. J. E., van Dijk, N. H., & Bruck, E. (2015). First-order ferromagnetic transition in single-crystalline (Mn,Fe)(2)( P,Si). *Journal of Materials Research*, 107(16), [162403]. <https://doi.org/10.1063/1.4934500>

### **Copyright**

Other than for strictly personal use, it is not permitted to download or to forward/distribute the text or part of it without the consent of the author(s) and/or copyright holder(s), unless the work is under an open content license (like Creative Commons).

### **Take-down policy**

If you believe that this document breaches copyright please contact us providing details, and we will remove access to the work immediately and investigate your claim.

*Downloaded from the University of Groningen/UMCG research database (Pure): <http://www.rug.nl/research/portal>. For technical reasons the number of authors shown on this cover page is limited to 10 maximum.*

# First-order ferromagnetic transition in single-crystalline $(\text{Mn,Fe})_2(\text{P,Si})$

H. Yibole,<sup>1,a)</sup> F. Guillou,<sup>1,2</sup> Y. K. Huang,<sup>3</sup> G. R. Blake,<sup>4</sup> A. J. E. Lefering,<sup>1</sup> N. H. van Dijk,<sup>1</sup> and E. Brück<sup>1</sup>

<sup>1</sup>FAME, TUDelft, Mekelweg 15, 2629JB Delft, The Netherlands

<sup>2</sup>ESRF, 71 Avenue des Martyrs, F-38043 Grenoble Cedex 09, France

<sup>3</sup>Van der Waals-Zeeman Instituut, Universiteit van Amsterdam, Science Park 904, 1098XH Amsterdam, The Netherlands

<sup>4</sup>Zernike Institute for Advanced Materials, University of Groningen, Nijenborgh 4, 9747 AG Groningen, The Netherlands

(Received 21 August 2015; accepted 11 October 2015; published online 22 October 2015)

$(\text{Mn,Fe})_2(\text{P,Si})$  single crystals have been grown by flux method. Single crystal X-ray diffraction demonstrates that  $\text{Mn}_{0.83}\text{Fe}_{1.17}\text{P}_{0.72}\text{Si}_{0.28}$  crystallizes in a hexagonal  $\text{Fe}_2\text{P}$  crystal structure (space group  $P\bar{6}2m$ ) at both 100 and 280 K, in the ferromagnetic and paramagnetic states, respectively. Magnetization measurements show that the crystals display a first-order ferromagnetic phase transition at their Curie temperature ( $T_C$ ). The preferred magnetization direction is along the  $c$  axis. A weak magnetic anisotropy of  $K_1 = 0.28 \times 10^6 \text{ J/m}^3$  and  $K_2 = 0.22 \times 10^6 \text{ J/m}^3$  is found at 5 K. A series of discontinuous magnetization jumps is observed far below  $T_C$  by increasing the field at constant temperature. These magnetization jumps are irreversible, occur spontaneously at a constant temperature and magnetic field, but can be restored by cycling across the first-order phase transition. © 2015 AIP Publishing LLC. [<http://dx.doi.org/10.1063/1.4934500>]

Only a few ferromagnets are known to exhibit a first-order magnetic transition (FOMT) at their  $T_C$ . Among those, the  $\text{Fe}_2\text{P}$ -based magnetocaloric materials have a rich and long history that dates back to the 1960s.<sup>1–4</sup> A great step towards a better understanding of this material was later made, thanks to the synthesis of high purity  $\text{Fe}_2\text{P}$  single crystals. It is now well accepted that  $\text{Fe}_2\text{P}$  is a ferromagnet with the easy direction along the  $c$  axis and that it shows a first-order ferromagnetic transition at  $T_C \approx 216 \text{ K}$ . However, a rare peculiarity is that the crystal symmetry does not change across the phase transition, as the space group remains  $P\bar{6}2m$ . Examples for this kind of iso-structural first-order transitions are scarce, and even more so when coupled with a change in magnetic order.

The manganese alloys derived from  $\text{Fe}_2\text{P}$  are currently attracting great interest as they display a giant magnetocaloric effect associated with a first-order magneto-elastic transition. This is of interest for many potential applications including magnetic refrigeration. Compared to the parent  $\text{Fe}_2\text{P}$ , the  $(\text{Mn,Fe})_2(\text{P,X})$  ( $\text{X} = \text{As, Ge, Si}$ ) materials are exceptional because they display a one order of magnitude more intense FOMT than  $\text{Fe}_2\text{P}$ , and their properties can be controlled by chemical substitutions.<sup>5–9</sup>

In spite of extensive experimental data on polycrystalline  $(\text{Mn,Fe})_2(\text{P,Si})$ , the understanding of the magnetic anisotropy and the field-induced metamagnetic transition in these materials is still limited. In particular, as the hexagonal structure is prone to cause anisotropy in the physical properties, a single crystal is required to obtain more detailed information. In this study, we report the crystal structure and magnetic properties of high purity single-crystalline  $(\text{Mn,Fe})_2(\text{P,Si})$ . This allows one to extend the insight obtained from previous observations made on polycrystalline

samples. In addition, a previously unknown magnetic behaviour related to the magnetization process at the ferro-to-paramagnetic FOMT is observed.

Single crystals of  $\text{Mn}_{0.83}\text{Fe}_{1.17}\text{P}_{0.72}\text{Si}_{0.28}$  were grown by the flux method with tin as a metallic flux. Numerous tests were performed to obtain the optimal conditions ensuring an appropriate silicon content. High-purity Mn (99.9%), Fe (99.9%), P (99.9%), and Si (99.999%) were used as starting materials. The starting materials of Mn, Fe, P, and Si with a nominal composition of  $\text{Mn}_{0.8}\text{Fe}_{1.2}\text{P}_{0.45}\text{Si}_{0.65}$  were mixed with high-purity Sn and then arc-melted under an Ar atmosphere in a water-cooled copper crucible. The resulting ingot was then sealed in a quartz ampoule in an Ar atmosphere of 200 mbar. The charge to flux ratio was 1:20 wt. %. The sealed ampoules were placed in a vertical furnace and heated to 1473 K in 6.5 h, maintained at this temperature for 100 h, and then cooled at a rate of 3 K/h to 700 K at which temperature the excess of tin was removed. When necessary, the remaining flux was removed by etching with diluted hydrochloric acid.

The chemical composition of the single crystal was determined by energy-dispersive X-ray spectroscopy (EDS) in a scanning electron microscope (SEM). The crystal structure was analysed with a single crystal X-ray diffraction (XRD) technique, and the magnetic properties were analyzed with SQUID magnetometry (see the supplementary material for details).<sup>10</sup>

In  $(\text{Mn,Fe})_2(\text{P,Si})$  materials, small deviations in the Mn/Fe and P/Si ratios can lead to very different crystal and magnetic properties. Due to the poor solubility of silicon in molten tin, the exact final compositions of the crystals are difficult to control. We noticed that by starting from nominal compositions with a relatively low silicon content ( $\text{Si} = 1/3$ ), the resulting  $\text{Mn}_{0.96}\text{Fe}_{0.94}\text{P}_{0.80}\text{Si}_{0.20}$  crystals are located at the boundary between orthorhombic ( $\text{Co}_2\text{P}$ -type) and

<sup>a)</sup>Electronic mail: Yibole@tudelft.nl

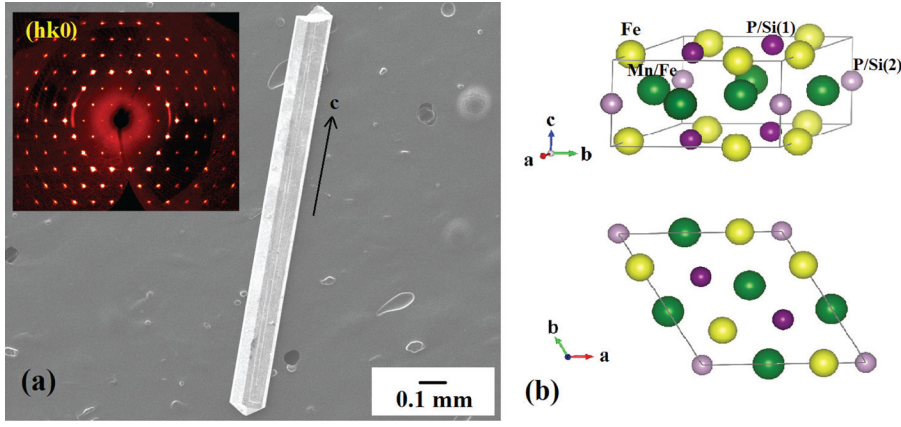


FIG. 1. (a) SEM image of as-grown  $\text{Mn}_{0.83}\text{Fe}_{1.17}\text{P}_{0.72}\text{Si}_{0.28}$  single crystals. The inset shows the experimental  $(h k 0)$  reciprocal lattice plane at 100 K. (b) Crystal structure.

hexagonal ( $\text{Fe}_2\text{P}$ -type) structures (see Figure S1 in the supplementary material).<sup>10</sup> This range corresponds to an antiferromagnetic order with a  $T_N \approx 120$  K. As we aimed to study the ferromagnetic transition, we will focus our attention in the rest of this letter on the crystals specifically grown with a larger Si content.

The as-grown crystals have a well-formed prismatic shape with average dimensions of about  $0.15 \times 0.15 \times 1.5 \text{ mm}^3$ . The surfaces of these crystals are regular and homogeneous. Figure 1(a) depicts one of the crystals as an example. The chemical formula for this crystal is  $\text{Mn}_{0.83}\text{Fe}_{1.17}\text{P}_{0.72}\text{Si}_{0.28}$ . Single crystal XRD was carried out at 280 K (paramagnetic phase) and 100 K (ferromagnetic phase) on a piece cut to dimensions of  $80 \times 80 \times 80 \mu\text{m}^3$ . The inset of Figure 1(a) shows the  $(h k 0)$  reciprocal lattice plane at 100 K. The data can be fitted using a structural model based on the  $\text{Fe}_2\text{P}$  structure. Structural refinements were carried out using 180 (100 K) and 182 (280 K) unique reflections having intensities  $I > 2\sigma$ . The chemical composition determined by EDS was used in the structural model. As represented in Figure 1(b), the tetrahedral  $3f$  position was filled by Fe atoms whereas the Mn atoms were set in the pyramidal  $3g$  position together with the remaining Fe atoms. The  $1b$  site was filled by P atoms, and the  $2c$  site contained both Si and the remaining P atoms. Since the  $P\bar{6}2m$  space group is non-centrosymmetric, the Flack parameter output by SHELXTL was used to determine the correct absolute structure. The possibility of inversion twinning was then checked during the refinement, but the twin fraction with the opposite absolute structure refined to zero within its standard error, indicating that the crystal piece used for XRD was of a single

domain. The refinements yielded low  $RF^2$  fit factors of 0.025 in both cases, demonstrating that the crystals are of single phase and of good quality. The lattice parameters for the ferromagnetic and paramagnetic states are listed in Table I. It should be noted that these values are for a crystal cycled across the phase transition (a comparison between the as-grown and cycled structures can be found in Table S1 in the supplementary material).<sup>10</sup> These diffraction data confirm the magneto-elastic character of the first-order transition. Across the FOMT, the space group remains  $P\bar{6}2m$ , and no un-indexed supplementary reflections are observed. However, crossing the ferromagnetic transition upon heating results in an expansion of the  $c$  axis and a contraction of the  $a$  axis, giving an increase in the  $c/a$  ratio of +5.3%. These results are in agreement with the previous report on polycrystals.<sup>7</sup>

Figure 2 presents the magnetization of  $\text{Mn}_{0.83}\text{Fe}_{1.17}\text{P}_{0.72}\text{Si}_{0.28}$  single crystal as a function of temperature for a magnetic field of 1 T. The inset shows the first cooling across the FOMT during which an extremely sharp increase in magnetization is observed, as most of the magnetization jump develops in a 1 K temperature increment. In polycrystalline materials, the  $T_C$  during the first cooling of an as-prepared sample is located at lower temperatures than for the subsequent measurement cycles. This phenomenon is called “virgin-effect,” which can be restored only by high-temperature annealing.<sup>11</sup> Here, a lower  $T_C$  is also observed

TABLE I. Lattice parameters and structure refinement of  $\text{Mn}_{0.83}\text{Fe}_{1.17}\text{P}_{0.72}\text{Si}_{0.28}$  from single crystal diffraction. Atomic positions:  $3g (x_1, 0, 1/2)$ ;  $3f (x_2, 0, 0)$ ;  $2c (1/3, 2/3, 0)$ , and  $1b (0, 0, 1/2)$ .

Temperature (K)	100	280
$a$ (Å)	6.0838(9)	5.997(6)
$c$ (Å)	3.3556(5)	3.484(3)
Volume (Å <sup>3</sup> )	107.56(4)	108.5(2)
$x_1$	0.5936(2)	0.5904(2)
$x_2$	0.2563(2)	0.2548(2)
Collected reflections	180	182
$RF^2$	0.0242	0.0243
Goodness-of-fit on $F^2$	1.096	1.050

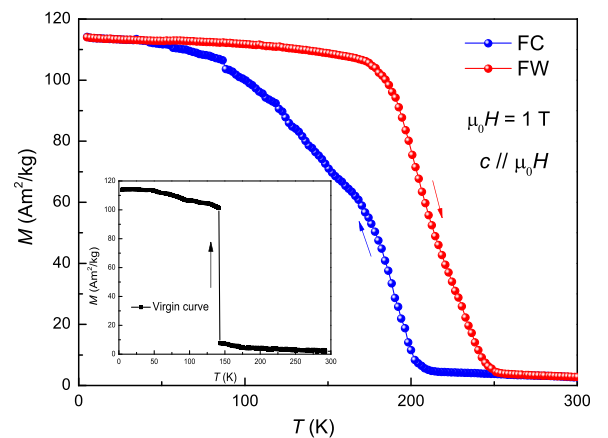


FIG. 2. Temperature dependence of the magnetization for  $\text{Mn}_{0.83}\text{Fe}_{1.17}\text{P}_{0.72}\text{Si}_{0.28}$ . The inset shows the first cooling curve (virgin curve) in similar conditions.

for the first cycle. The subsequent heating and cooling curves present a much broader transition at  $T_C = 210$  and 170 K (defined as the center of the  $|\frac{dM}{dT}|$  peak at 50 mT) for heating and cooling, respectively. Such a large thermal hysteresis of 40 K demonstrates the first-order character of this magneto-elastic phase transition.

The magnetic anisotropy of the  $\text{Mn}_{0.83}\text{Fe}_{1.17}\text{P}_{0.72}\text{Si}_{0.28}$  crystal (after field cycling at 5 T) was investigated by measuring the isothermal magnetization along the  $c$  axis and in the basal ( $a, b$ ) plane. For the field direction perpendicular to the long axis of the crystal, the magnetic field was corrected by using a demagnetization factor of  $N = 1/2$ . The results are shown in Figure 3 and compared with the magnetization curve for a polycrystal of identical nominal composition. For a magnetic field parallel to the crystallographic  $c$  axis, the magnetization increases very rapidly and saturates at fields lower than 1 T. On the other hand, a significantly larger field is needed to reach saturation in the field direction perpendicular to the  $c$  axis. The saturation magnetization is  $4.5 \mu_B$  at 5 K, which is slightly higher than that of the polycrystalline sample. This discrepancy can be explained by the presence of a small amount of impurity phase with a lower magnetization in the polycrystals and by the uncertainty involved in determining the single crystal mass. The saturation magnetization of the single crystal is consistent with previous reports on closely related compositions on the basis of bulk magnetometry and neutron diffraction.<sup>12</sup> Here, we can estimate the magnetic anisotropy quantitatively. As usual for a hexagonal system, we consider only the first and second-order anisotropy constants for the magnetocrystalline anisotropy energy  $E \approx K_1 \sin^2 \theta + K_2 \sin^4 \theta$ , where  $\theta$  is the polar angle between the  $c$  axis and the magnetization vector. The magnetocrystalline anisotropy constants are deduced using the method developed by Sucksmith and Thompson.<sup>13</sup> The resulting values are  $K_1 = 0.28 \times 10^6 \text{ J/m}^3$  and  $K_2 = 0.22 \times 10^6 \text{ J/m}^3$  at 5 K. This shows that  $K_1$  is predominant and positive. Thus, the preferred magnetization direction in  $\text{Mn}_{0.83}\text{Fe}_{1.17}\text{P}_{0.72}\text{Si}_{0.28}$  crystals is along the  $c$  axis. This is consistent with the results from an earlier neutron diffraction study that shows the easy magnetization direction in

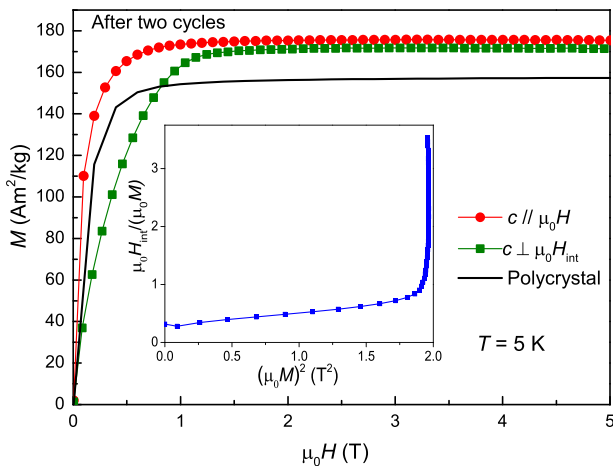


FIG. 3. Field dependence of the magnetization for single-crystalline and polycrystal  $\text{Mn}_{0.83}\text{Fe}_{1.17}\text{P}_{0.72}\text{Si}_{0.28}$ . The inset shows the Sucksmith-Thompson plot derived from the  $M(H)$  curve with field applied perpendicular to the  $c$  axis, i.e., the solid square in main panel.

$\text{MnFe}(\text{P}_{1-x}\text{Si}_x)$  compounds lies close to the  $c$  axis, with an angle of  $\theta = 29^\circ$  for  $x = 0.34$ .<sup>12</sup> It is interesting to note that for  $\text{MnFe}(\text{P}, \text{Ge})$  materials, the magnetic moments lay in the ( $a, b$ ) plane.<sup>14</sup> The anisotropy constants above are one order of magnitude lower than those found for the parent compound  $\text{Fe}_2\text{P}$ .<sup>3,15</sup> For magnetocaloric applications, it is of importance to reach a high degree of alignment of the magnetic moment at a magnetic field as low as possible. In this respect, the weakening of the magnetic anisotropy from  $\text{Fe}_2\text{P}$  to  $(\text{Mn}, \text{Fe})_2(\text{P}, \text{Si})$  materials is beneficial.

Figure 4 shows the initial  $M(H)$  curves taken prior to the data presented in Figure 3 after zero-field cooling (ZFC). In Figure 4(a), as the field is increased for the first time, a plateau of almost constant magnetization ( $113 \text{ Am}^2 \text{ kg}^{-1}$ ) is observed until around 3 T, in agreement with the  $M(T)$  measurement shown in Figure 2. Above 3 T, a series of step-like magnetization jumps occurs. These unusual magnetization jumps also occur along the direction perpendicular to the  $c$  axis, as shown in Figure 4(b). We note that the data in Fig. 4(b) were measured prior to those in Fig. 4(a). Although the magnetic field must be above a certain threshold for the jumps in magnetization to fully develop, they do not occur at regular field intervals. Steps in magnetization in the opposite direction were never observed during demagnetization from 5 T to zero magnetic field, or in subsequent magnetization/demagnetization cycles (at constant temperature), as shown in Figs. 4(a) and 4(b). As the initial field-increase  $M(H)$  curves in Figs. 4(a) and 4(b) were measured with a ZFC history, the present magnetization jumps observed in single crystals do *not* correspond to the usual virgin effect previously reported in polycrystals, as this disappears after one instance of thermal cycling. Here, in our single crystals, the

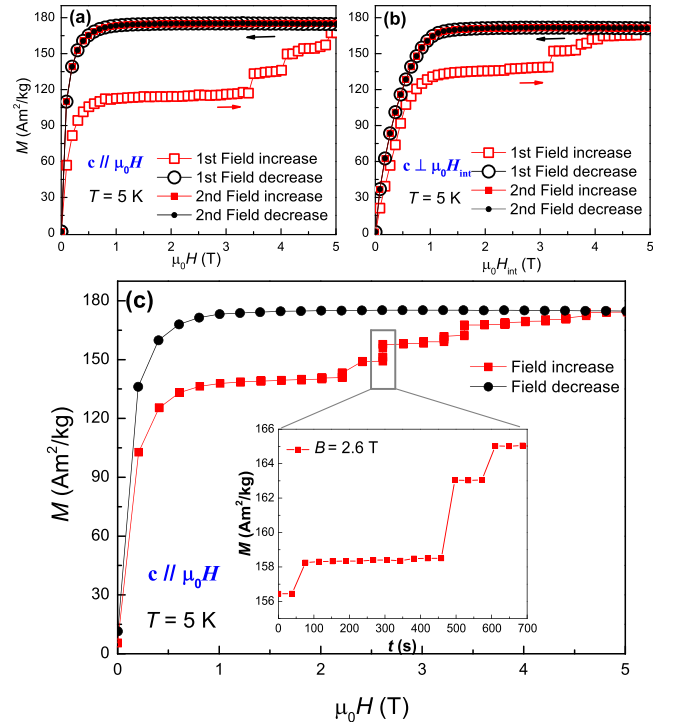


FIG. 4. (a) and (b) Field dependence of the magnetization for single-crystalline  $\text{Mn}_{0.83}\text{Fe}_{1.17}\text{P}_{0.72}\text{Si}_{0.28}$  at 5 K after ZFC for two principal directions. (c) Magnetization as a function of field. The inset shows the enlargement of the magnetic relaxation for the magnetic field of 2.6 T.



magnetization jumps can be recovered after “resetting” the materials by cycling across the FOMT. However, after many thermal cycles ( $n > 5$ ), or when the cooling is carried out in different magnetic field ( $H \neq 0$ ), we observed that the field required to induce the magnetization jumps varies, indicating that this phenomenon is sensitive to the thermal and magnetic history.

To check whether these magnetization jumps are related to dynamic effects during the magnetization process, we measured the magnetic relaxation at 5 K for the  $\text{Mn}_{0.83}\text{Fe}_{1.17}\text{P}_{0.72}\text{Si}_{0.28}$  crystal, at each magnetic field during magnetization from zero to 5 T (after a ZFC). As shown in Figure 4(c), the magnetization jumps occur spontaneously at a constant temperature and magnetic field. In the inset of Figure 4(c), several magnetization plateaus separated by steps can be distinguished during a single relaxation curve. Such a feature is rather uncommon for related systems. These results show a strong time-dependent effect and indicate the existence of several non-equilibrium metastable states. The time scale of these magnetization jumps (several hundred seconds after applying the magnetic field) and the magnetic field range ( $> 2.5$  T) indicates that we are dealing with a phenomenon related to the phase transition, and not with more generic magnetization processes such as eddy currents (much smaller time scale) or domain wall movements (relevant at lower magnetic field).

Such a step-like magnetic behaviour is previously unknown in  $(\text{Mn,Fe})_2(\text{P,Si})$  compounds. We believe that two mechanisms could contribute to it: (i) an underlying antiferromagnetic order and (ii) a dynamical phase separation phenomenon. The first interpretation is specific to  $(\text{Mn,Fe})_2(\text{P,Si})$  materials. In  $\text{FeMnP}_{0.75}\text{Si}_{0.25}$  polycrystalline samples, it has recently been found that, in neutron diffraction experiments and first principles calculations, ferromagnetism and a metastable antiferromagnetic phase can coexist below  $T_C$ .<sup>16,17</sup> These observations were made for samples on the Si-poor edge of the phase diagram, which is close to the composition of our single crystals. The development of an intermediate metastable antiferromagnetic state when crossing the high temperature paramagnetic to ferromagnetic state is expected to be promoted by chemical disorder on the 3f and 3g sites. In this context, the magnetization jumps would correspond to a partial field induced antiferromagnetic-to-ferromagnetic transition. The second mechanism is more general to a FOMT. Similar behaviour involving successive magnetic discontinuities associated with a FOMT has been observed in a wide variety of materials.<sup>18–23</sup> Depending on the system, different interpretations have been proposed. The most frequent explanation is the so-called martensitic scenario.<sup>18,19</sup> This relies on the fact that the two magnetic phases at play correspond to two incompatible crystallographic phases (either with different lattice symmetry or different cell parameters), so that the growth of one phase occurs at the expense of the other and will result in interfacial strain. Upon cooling across the FOMT, the interfacial strain created at the interface between the ferromagnetic phase and a less magnetic phase (paramagnetic or antiferromagnetic due to the aforementioned mechanism) with different cell parameters will result in an arrest of the transition. A fraction of the crystal will be blocked in a metastable low

magnetization state far below the equilibrium  $T_C$ . At low temperatures, as the magnetic field is increased, the driving force aligning the spins becomes strong enough to overcome the energy barrier from the interfacial strain; thus, the ferromagnetic phase experiences a burst-like growth and leads to a magnetization jump. It is possible that the resolution of our XRD technique is insufficient to detect a nanoscale phase separation. Better spatial resolution such as that provided by TEM or nanotomography is required to investigate the distribution of the different phases in the crystal.

To conclude,  $(\text{Mn,Fe})_2(\text{P,Si})$  single crystals presenting a first-order ferromagnetic-to-paramagnetic transition have been grown. Our studies of their structural and magnetic properties support the findings of previous works on polycrystalline materials. A weak magnetic anisotropy is found at 5 K, indicating a soft magnetic behaviour favourable for magnetic refrigeration. The magnetization process toward the ferromagnetic state turns out to be more complex in the single crystals than for the polycrystalline samples. A series of discontinuous magnetization jumps can be observed far below the Curie temperature. These jumps are irreversible, but can be restored by thermally cycling and thus “resetting” the crystal across the FOMT.

The authors would like to thank Bert Zwart for his help in sample preparation. This work was financially supported by the Foundation for Fundamental Research on Matter (FOM) (The Netherlands) and BASF New Business.

<sup>1</sup>S. Rundqvist and F. Jelinek, *Acta Chem. Scand.* **13**, 425 (1959).

<sup>2</sup>A. R. R. Fruchart and J. P. Senateur, *J. Appl. Phys.* **40**, 1250 (1969).

<sup>3</sup>H. Fujii, T. Hkabe, T. Kamigaichi, and T. Okamoto, *J. Phys. Soc. Jpn.* **43**, 41 (1977).

<sup>4</sup>L. Lundgren, G. Tarmohamed, O. Beckman, B. Carlsson, and S. Rundqvist, *Phys. Scr.* **17**, 39 (1978).

<sup>5</sup>O. Tegus, E. Brück, K. H. J. Buschow, and F. R. de Boer, *Nature* **415**, 150 (2002).

<sup>6</sup>N. T. Trung, Z. Q. Ou, T. J. Gortenmulder, O. Tegus, K. H. J. Buschow, and E. Brück, *Appl. Phys. Lett.* **94**, 102513 (2009).

<sup>7</sup>N. H. Dung, Z. Q. Ou, L. Caron, L. Zhang, D. T. C. Thanh, G. A. de Wijs, R. A. de Groot, K. H. J. Buschow, and E. Brück, *Adv. Energy Mater.* **1**, 1215 (2011).

<sup>8</sup>H. Yibole, F. Guillou, L. Zhang, N. H. van Dijk, and E. Brück, *J. Phys. D: Appl. Phys.* **47**, 075002 (2014).

<sup>9</sup>F. Guillou, G. Porcari, H. Yibole, N. van Dijk, and E. Brück, *Adv. Mater.* **26**, 2671 (2014).

<sup>10</sup>See supplementary material at <http://dx.doi.org/10.1063/1.4934500> for details of experimental techniques, single crystal XRD data for as-grown and cycled single crystal, and antiferromagnetic  $(\text{Mn,Fe})_2(\text{P,Si})$  crystal.

<sup>11</sup>X. F. Miao, L. Caron, Z. Gercsi, A. Daoud-Aladine, N. H. van Dijk, and E. Brück, *Appl. Phys. Lett.* **107**, 042403 (2015).

<sup>12</sup>Z. Ou, L. Zhang, N. Dung, L. van Eijck, A. Mulders, M. Avdeev, N. van Dijk, and E. Brück, *J. Magn. Magn. Mater.* **340**, 80 (2013).

<sup>13</sup>W. Sucksmith and J. E. Thompson, *Proc. R. Soc. A* **225**, 362 (1954).

<sup>14</sup>D. Liu, M. Yue, J. Zhang, T. M. McQueen, J. W. Lynn, X. Wang, Y. Chen, J. Li, R. J. Cava, X. Liu, Z. Altounian, and Q. Huang, *Phys. Rev. B* **79**, 014435 (2009).

<sup>15</sup>L. Caron, M. Hudl, V. Högl, N. H. Dung, C. P. Gomez, M. Sahlberg, E. Brück, Y. Andersson, and P. Nordblad, *Phys. Rev. B* **88**, 094440 (2013).

<sup>16</sup>V. Högl, M. Hudl, L. Caron, P. Beran, M. H. Sørby, P. Nordblad, Y. Andersson, and M. Sahlberg, *J. Solid State Chem.* **221**, 240 (2015).

<sup>17</sup>G. Li, W. Li, S. Schönecker, X. Li, E. K. Delczeg-Czirjak, Y. O. Kvashnin, O. Eriksson, B. Johansson, and L. Vitos, *Appl. Phys. Lett.* **105**, 262405 (2014).

<sup>18</sup>R. Mahendiran, A. Maignan, S. Hébert, C. Martin, M. Hervieu, B. Raveau, J. F. Mitchell, and P. Schiffer, *Phys. Rev. Lett.* **89**, 286602 (2002).

- <sup>19</sup>V. Hardy, S. Majumdar, S. J. Crowe, M. R. Lees, D. M. Paul, L. Hervé, A. Maignan, S. Hébert, C. Martin, C. Yaicle, M. Hervieu, and B. Raveau, *Phys. Rev. B* **69**, 020407 (2004).
- <sup>20</sup>V. Hardy, A. Maignan, S. Hébert, C. Yaicle, C. Martin, M. Hervieu, M. R. Lees, G. Rowlands, D. M. K. Paul, and B. Raveau, *Phys. Rev. B* **68**, 220402 (2003).
- <sup>21</sup>A. Haldar, K. G. Suresh, and A. K. Nigam, *Phys. Rev. B* **78**, 144429 (2008).
- <sup>22</sup>S. N. Jammalamadaka, N. Mohapatra, S. D. Das, K. K. Iyer, and E. V. Sampathkumaran, *J. Phys.: Condens. Matter* **20**, 425204 (2008).
- <sup>23</sup>S. B. Roy, M. K. Chattopadhyay, P. Chaddah, and A. K. Nigam, *Phys. Rev. B* **71**, 174413 (2005).